

Nanophotonic trapping for precise manipulation of biomolecular arrays

Mohammad Soltani^{1,2†}, Jun Lin^{1,2†}, Robert A. Forties^{1,2}, James T. Inman¹, Summer N. Saraf¹, Robert M. Fulbright¹, Michal Lipson^{3,4} and Michelle D. Wang^{1,2*}

Optical trapping is a powerful manipulation and measurement technique widely used in the biological and materials sciences^{1–8}. Miniaturizing optical trap instruments onto optofluidic platforms holds promise for high-throughput lab-on-a-chip applications^{9–16}. However, a persistent challenge with existing optofluidic devices has been achieving controlled and precise manipulation of trapped particles. Here, we report a new class of on-chip optical trapping devices. Using photonic interference functionalities, an array of stable, three-dimensional on-chip optical traps is formed at the antinodes of a standing-wave evanescent field on a nanophotonic waveguide. By employing the thermo-optic effect via integrated electric microheaters, the traps can be repositioned at high speed (~ 30 kHz) with nanometre precision. We demonstrate sorting and manipulation of individual DNA molecules. In conjunction with laminar flows and fluorescence, we also show precise control of the chemical environment of a sample with simultaneous monitoring. Such a controllable trapping device has the potential to achieve high-throughput precision measurements on chip.

A prominent example of the application of optical trapping techniques is the vibrant area of biophysics, in which the mechanical behaviour of biological molecules can be investigated at the single-molecule level^{2–4}. It is now possible to disrupt protein complexes with piconewton forces and track motor proteins with nanometre and millisecond resolution. However, conventional optical trapping instruments are only capable of manipulating one molecule at a time, which limits their throughput. Methods for generating multiple optical traps via time-sharing of a single laser beam¹⁷ or holographic modulation¹⁸ have the drawback of requiring proportionally increased laser power. For optical trapping to realize its full potential, a new platform is needed to enable manipulation with high resolution and high throughput.

Optical trapping based on photonic structures in an optofluidic platform presents a potential solution to these drawbacks. The strong gradient in the evanescent fields of these structures can trap and transport a large array of particles, even at low optical powers^{9–12,19–27}. Despite recent advances, no device has achieved stable three-dimensional trapping with controllable repositioning, features that are essential for manipulation.

Here, we present a platform enabling high-throughput three-dimensional optical trapping with precision manipulation on chip. The core component of the device is a standing-wave interferometer (Fig. 1a,b), where light in a waveguide is split into two arms of equal light intensity and the two arms are then joined, leading to interference of two counter-propagating waves and therefore the formation of a standing wave. Thus, in the portion of the waveguide exposed to fluid (Fig. 1c), stable three-dimensional optical traps are

formed by the evanescent field at the antinodes of the standing wave. We refer to this type of device as a nanophotonic standing-wave array trap (nSWAT). In a conventional optical trap, a single laser beam typically traps only one particle, so the laser power must be increased in proportion to the number of traps. In contrast, in an nSWAT, the same laser beam is ‘recycled’ to form an array of periodically spaced traps, so a large number of traps can be formed, each with stiffness comparable to that of a conventional optical trap (Supplementary Fig. 1), and without the need to increase the laser power.

In an nSWAT, the entire trapping array can be precisely repositioned by controlling the phase difference of the counter-propagating waves. This phase difference is achieved by using an integrated electric microheater that heats part of the waveguide, inducing a phase change via the thermo-optic effect^{27,28} (Supplementary Fig. 2). To suspend and manipulate single DNA molecules we incorporated two copies of an nSWAT in a single device, each controlled independently by its own microheater. The power from an incoming laser beam was divided between the two nSWATs by a Mach–Zehnder interferometer (MZI) switch, which was controlled by a third integrated electric microheater to allow sorting.

An nSWAT is naturally stable because all optical elements creating the traps are on chip with a short path difference (~ 100 μm) between the counter-propagating waves. Such stable trapping is essential for precision measurements of molecular events. By contrast, in a conventional benchtop optical trap, drift is inevitable and must be minimized using elaborate measures^{29,30}. To demonstrate the inherent stability of an nSWAT we held a bead in a trap of an nSWAT and monitored its position over time relative to the waveguide by means of video tracking (see Methods). Figure 2a shows that the bead had no discernible drift relative to the waveguide for over 10 min. In addition to stability, we also demonstrated that nSWATs are exceptionally resistant to environmental noise and vibrations (Supplementary Fig. 3). Thus, nSWATs are ideally suited to long-term, low-noise measurements, with no need for extensive drift reduction and vibration isolation.

Here, we demonstrate the nanometre resolution control of the positioning of trapped beads using an nSWAT. To determine how well a trapped bead can be positioned, we applied a square-wave voltage to the microheater while simultaneously measuring the position of the trapped bead. As shown in Fig. 2b, 10 nm steps are readily resolved, and even 2 nm steps are discernible, indicating the potential of this device for detecting molecular events that occur at the nanometre scale³¹.

We also demonstrate a method for precision transport of trapped particles over many micrometres using an nSWAT without applying damagingly high voltage to the microheater (Fig. 3). To do this, we took advantage of the periodic spacing of the traps. The positioning

¹Department of Physics—Laboratory of Atomic and Solid State Physics, Cornell University, Ithaca, New York 14853, USA. ²Howard Hughes Medical Institute, Cornell University, Ithaca, New York 14853, USA. ³Department of Electrical and Computer Engineering, Cornell University, Ithaca, New York 14853, USA.

⁴Kavli Institute at Cornell University, Ithaca, New York 14853, USA. [†]These authors contributed equally to this work. *e-mail: mwang@physics.cornell.edu

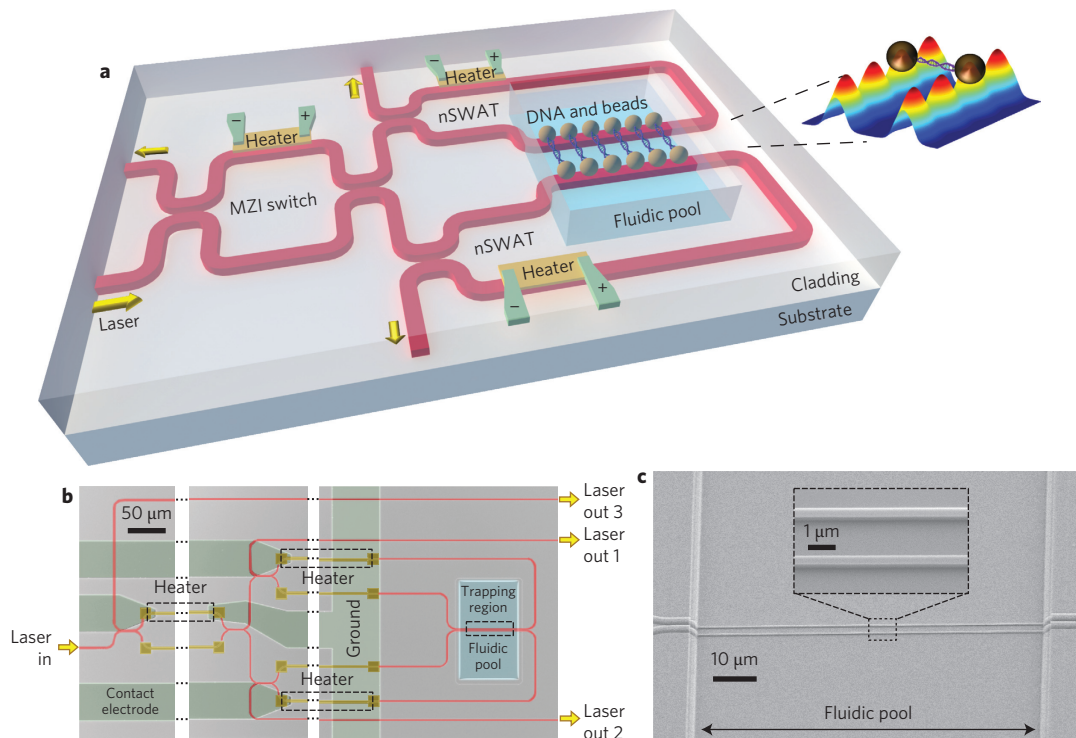


Figure 1 | Design and fabrication of an nSWAT device. **a**, Schematic of device design. nSWATs were implemented with silicon waveguides on a silicon-on-insulator (SOI) platform (see Methods). Laser input to the waveguide is partitioned into two nSWATs using a Mach-Zehnder interferometer (MZI). nSWATs have a 50/50 waveguide beamsplitter with output arms connected to generate counter-propagating waves. Three microheaters are located above the waveguides, one in the MZI to control partitioning of the laser into the two nSWATs and two more to control the trap positions in each nSWAT. The microheaters and waveguides are buried in oxide, except for the exposed waveguides in the fluidic pool trapping region. Inset: Array of traps with a DNA molecule suspended between two beads held by nSWATs. The coloured three-dimensional plot shows the calculated energy density of standing waves on both waveguides (Supplementary Fig. 1). **b**, Optical microscope image of the fabricated device (false coloured). Each microheater is located on one of the two arms after a splitter, while an unconnected strip of metal is located on the other arm to balance the potential optical loss introduced by the metal in the proximity of the waveguide. The waveguides are made of silicon on a SOI wafer. **c**, Scanning electron micrograph of the waveguides in the trapping region. The waveguides are 440 nm in width and 250 nm in height. Note that, although all waveguides reside in the same plane, the protective layer of oxide outside the fluid channel gives the illusion that they do not by amplifying the structure of the underlying waveguides.

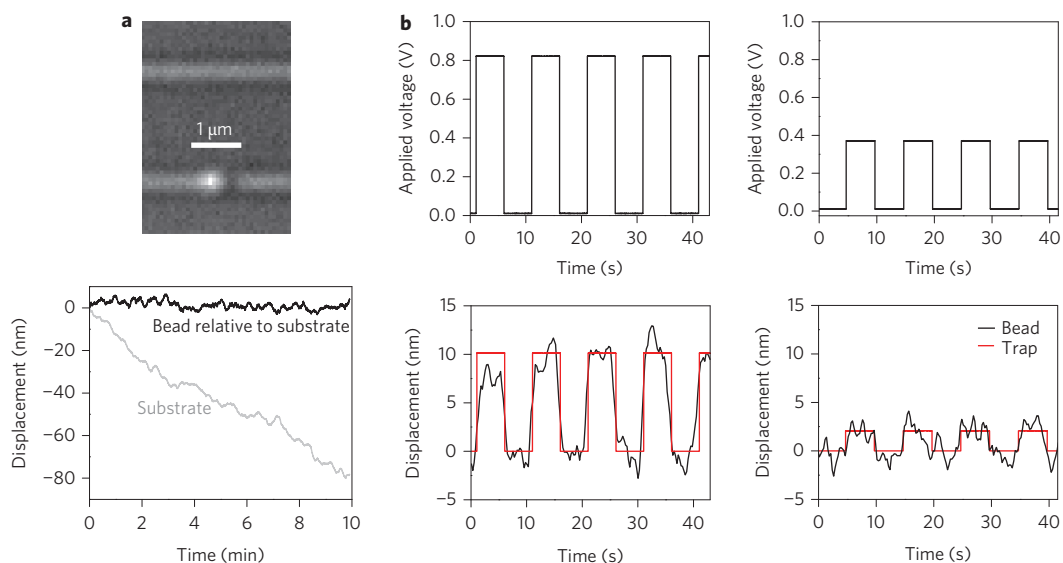


Figure 2 | Trapping stability and resolution. **a**, Trapping stability measurements. Top: Optical microscope image of a bead (490 nm in diameter) held on the lower nSWAT. Bottom: Bead position along the waveguide, relative to the waveguide, over 10 min. The oxide edge of the fluid region on the device was used as a fiducial marker. **b**, Trapping control resolution. The position of a bead held by an nSWAT was measured as the trap was stepped in a square-wave fashion by the application of a voltage to the microheater to generate 10 nm (left) and 2 nm (right) steps. Red curves are fits to a periodic square wavefunction, with the amplitude, period and phase delay as fitting parameters.

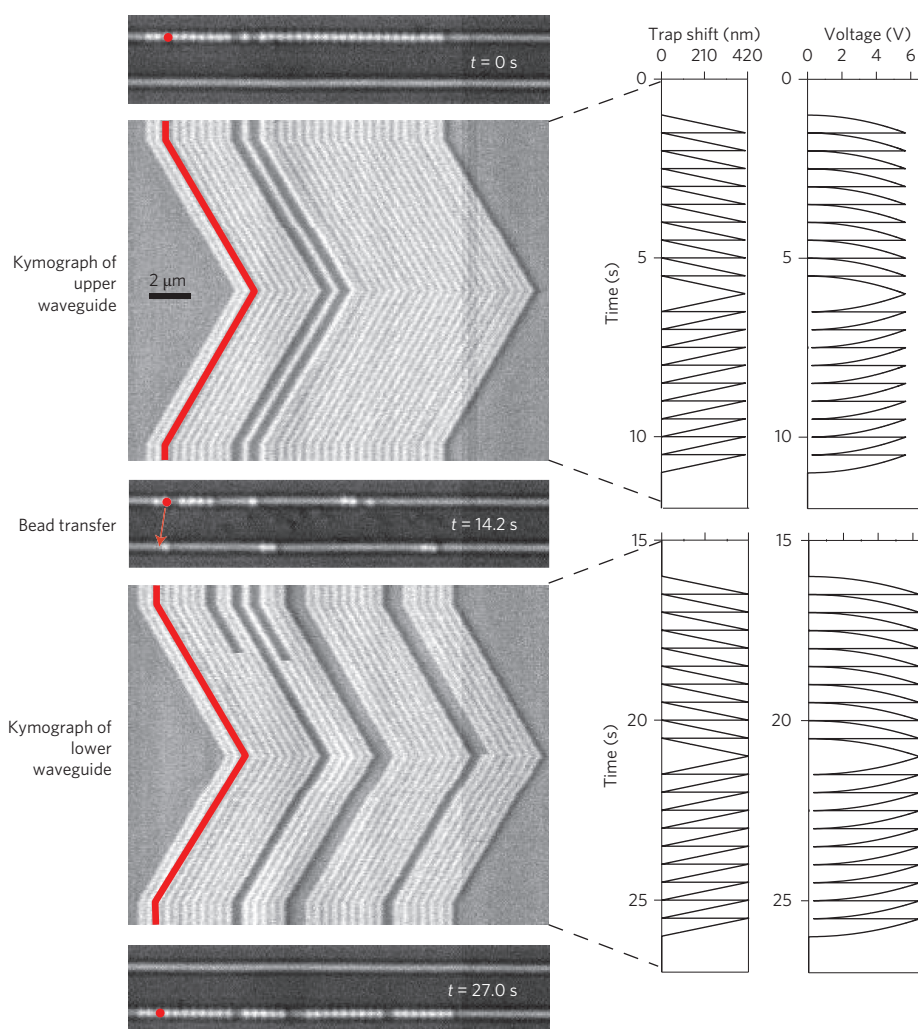


Figure 3 | Controlled long-range transportation by an nSWAT. An array of beads (356 nm in diameter, one false coloured) were initially trapped on the upper waveguide and transported in a controlled manner along the waveguide in both directions (Supplementary Movie 1). Subsequently, laser power was switched from the upper to the lower waveguide using the MZI switch, and beads were then trapped and transported along the lower waveguide. Each kymograph shows a line scan of an image of the active waveguide (horizontal axis) versus time (vertical axis), with the corresponding voltage applied to the microheater and the resulting phase shift of the standing wave plotted on the right.

of the nSWATs was precisely calibrated (Supplementary Fig. 2) so that by applying a nonlinear increasing voltage ramp to the microheater of an nSWAT (Fig. 3) a linear ramp in the trap array position was generated to steadily displace the array by one spatial period of the standing wave (~ 430 nm; see Methods). The voltage was then reset to zero and the ramping process was repeated, resulting in a sawtooth pattern in the trap array position. Because the trap array was reset much faster (~ 30 kHz, Supplementary Fig. 4) than the corner frequency of a trapped bead (150 Hz, Supplementary Fig. 1), the bead could not respond to the sudden trap position reset and instead behaved as if the microheater voltage was ramped continuously (see Methods). This resulted in a steady movement of trapped beads at a constant controlled speed, with the transport distance limited only by the size of the trapping region. Figure 3 shows an example of this long-distance transport of an array of beads (Supplementary Movie 1). This array was initially trapped on the upper waveguide and was transported at a constant speed over several micrometres, in both directions. The laser power was then switched from the upper to the lower waveguide using the MZI switch microheater. At this point, a modest fluid flow was applied to direct the motion of the beads downward, and the array of trapped beads was shifted to the lower waveguide. The beads were

then transported along the lower waveguide. Note that the spacing of the beads in this packed array corresponds well with the expected periodicity of the standing wave (Supplementary Fig. 5).

As an application of nSWAT to biomolecules we demonstrate sorting of DNA dumbbells—single molecules of DNA with a bead attached at each end³²—from a mixture of other bead and DNA species (see Methods), and also the subsequent manipulation of these DNA dumbbells. Sorting is often a critical priming step for single-molecule measurements. Here, sorting was achieved by switching off the optical trapping force in one waveguide while applying a modest flow to direct motion of the released particles away from the other waveguide (Fig. 4a and Supplementary Movie 2). Trapping by the upper waveguide in the presence of downward fluid flow revealed DNA dumbbells. Subsequent trapping by the lower waveguide in the presence of upward flow retained the DNA dumbbells and removed all other trapped bead species. This process may be repeated for further enrichment of DNA dumbbells. Subsequently, the array of DNA molecules was extended by moving the traps of the lower nSWAT relative to those of the upper nSWAT. We envision that this sorting and stretching ability would be advantageous in various situations. For example, DNA may be suspended between the two waveguides for visualization

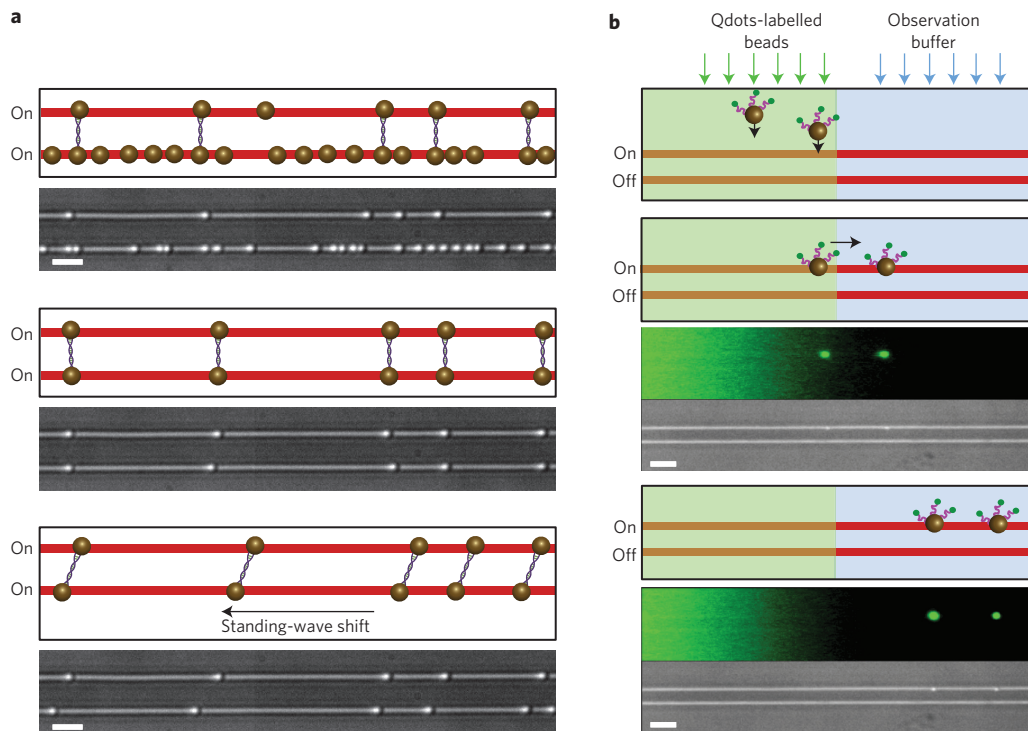


Figure 4 | Manipulation, transport and change of chemical environment of biomolecules. **a**, Sorting and manipulation of individual DNA molecules. Cartoons and corresponding movie frames (Supplementary Movie 2) explain the steps in the process. DNA dumbbells were formed using beads of 490 nm diameter and sorted by a combination of trapping and fluid flow forces. The sorted array of DNA dumbbells was extended by moving the traps of the lower nSWAT relative to those of the upper nSWAT. Scale bars, 2 μm . **b**, On-chip changes of the chemical environment of the biomolecules with simultaneous fluorescence monitoring. Cartoons and corresponding movie frames (Supplementary Movie 3) explain the steps in the process. Each movie frame is composed of two panels, with the upper panel showing a fluorescence image and the lower showing the corresponding bright-field image. Free Qdots and Qdot-labelled beads were introduced by the left laminar flow. The cartoons show only beads (brown) labelled with Qdots (green) via DNA linkers (purple). Beads were trapped by the upper nSWAT and subsequently transported to and held in the right laminar flow (observation buffer), which had a different chemical environment. During the experiment, the lower nSWAT was off. Scale bars, 4 μm .

of motor protein movement along the DNA, complexes bound to the DNA may be disrupted by stretching the DNA, or enriched DNA dumbbells may be transported to a different region for a chemical or biomolecular reaction.

As another application of nSWAT to biochemical experiments, we demonstrate how a bead-bound sample can be transported from one chemical environment to another, potentially for a sequence of chemical reactions and analyses, all on chip (Fig. 4b and Supplementary Movie 3; see Methods). We formed two adjacent laminar flows over the waveguides, with one laminar flow containing a mixture of free quantum dots (Qdots) and Qdot-labelled beads, and the other containing observation buffer. Only beads were trapped by an nSWAT. They were then transported to the adjacent laminar flow (observation buffer) and held briefly to simulate a potential reaction and/or measurement before release. We envision this technology will enable many potential applications for on-chip sorting, sampling and monitoring of biochemical reactions.

In conclusion, we have demonstrated a new platform for the next generation of optical trapping instruments. This platform has a number of advantages. First, it enables high throughput, as tens or potentially hundreds of trapped particles can be monitored and manipulated at the same time. Second, this multiplexing is achieved using laser power comparable to that of a single optical trap, in contrast to conventional microscope-based multiplexing approaches. Third, the on-chip nature of our device makes it inherently stable, eliminating the need for complicated drift-reduction techniques. Finally, the horizontal geometry and ultrafast trap control are well suited for integration with fluorescence and laminar flow channels. Although in this work the nSWAT device was implemented with

silicon waveguides, it can be realized with different optical materials and at different wavelength ranges. We envision that our instrument will enable routine high-throughput optical-trapping experiments for biophysical and biochemical analysis. Thus, the nSWATs establish parallel processing and promise to make manipulation and precision measurements broadly available.

Methods

Device fabrication and characterization. The device fabrication process is similar to (and modified from) one we have described previously²⁷. Details can be found in Supplementary Section 1. For device characterization, a tunable laser (at 1,550 nm, Ando AD4321Q), after amplification by a laser amplifier (IPG Photonics), was coupled to the chip using an optical tapered lensed fibre. A fibre polarization controller adjusted the light polarization to the transverse-magnetic polarization mode of the waveguide. The transmitted light through the chip was collected from the opposite end of the chip using an additional tapered lensed optical fibre and sent to a photodetector (Thorlabs, PDB150C). A microprobe (GGB Industries) for applying electric voltage was connected to the contact electrodes of the microheater (with a measured resistance of $\sim 300 \Omega$). The optimal operational wavelength range occurs when minimum light is transmitted through the output port of the nSWAT to the photodetector. This means that a standing wave made of counter-propagating waves with nearly equal amplitudes has been formed in the trapping region. In all the experiments described in this Letter, the laser power in the trapping region was 30–40 mW for all measurements, except for calibrations.

Trapping methods. To prevent beads from sticking to the device surfaces we coated the sample chamber with 1 mg ml^{-1} 1, 2-dioleoyl-*sn*-glycero-3-phosphocholine (DOPC) in 100 mM NaCl and 10 mM Tris pH 8.0. For trapping experiments, polystyrene beads (Polysciences) with diameters of 356 nm or 490 nm in 20 mM Tris-HCl pH 8.0 were flowed into the microfluidic channel using syringe pumps (Harvard PhD 2000). Using image tracking (see next section), the spacing between traps in the nSWAT was determined experimentally to be 423 nm (Fig. 3, Supplementary Fig. 5).

To ensure continuous long-distance transport, as shown in Fig. 3, a trapped bead should not move substantially during the brief reset of the microheater voltage

(~30 μ s, Supplementary Fig. 4). For simplicity, we assumed that the bead undergoes diffusion during the voltage reset, so the distance it diffuses during the reset will be ~15 nm, smaller than the amplitude of its Brownian motion in a stationary trap (~20 nm) (Supplementary Fig. 1). Even if the bead is subjected to an external force during the reset (for example, 1 pN), its biased motion is still limited (~9 nm displacement along the direction of the force). Therefore, because the voltage reset is rapid, the bead effectively remains stationary during the reset and is transported smoothly without interruption.

Imaging and tracking of trapped beads. The sample plane was imaged by a $\times 100$, 1.3 NA oil-immersion objective (Nikon) using a charge-coupled device (CCD) camera (JAI RM-6740GE, 7.4 μ m pixel). Bead positions were determined by fitting a circular Gaussian spot to the image of each bead in each frame³³. This allowed us to localize a bead to better than 10 nm using one frame, and higher resolution was achieved by averaging over multiple frames. For stability measurements (Fig. 2a), images were acquired at 10 frames per second (f.p.s.), then the data were averaged to 0.1 f.p.s., while stepping measurements (Fig. 2b) were acquired at 540 f.p.s. and averaged to 10.8 f.p.s. To correct for drift of the sample relative to the camera, we also tracked the position of one edge of the fluidic pool and subtracted this displacement from all measured bead displacements.

Preparation of DNA. The 10 kbp DNA template used in the experiments was prepared using methods similar to those described previously^{34,35}. Briefly, a 10 kbp plasmid (available upon request) was cut with SspI (NEB) to produce nonpalindromic overhangs. A fill-in reaction with Klenow fragment (NEB), digoxigenin-11-dUTP and biotin-11-dATP (Roche) was used to label the linearized plasmid DNA. This resulted in one end of the DNA being labelled with digoxigenin and the other with biotin. A similar method was used to prepare the 30 bp DNA used for Qdot-labelling.

Preparation of DNA-tethered beads. To form DNA dumbbells, 10 kbp DNA was mixed with both 490 nm streptavidin-coated beads and anti-digoxigenin-coated beads at a molar ratio of 3:1:1 following a previously described protocol³⁴.

Preparation of Qdot-labelled beads. To form Qdot-labelled beads, Qdot 525 streptavidin conjugate (Invitrogen) was mixed with 490 nm anti-digoxigenin-coated polystyrene beads and a 30 bp DNA with biotin label at one end and digoxigenin label at the other, following previously described protocols³⁴. Laminar flow was established by multiple inlets to our flow cells. The relative size of each flow was controlled by adjusting the inlet pressures. The outlet flow rate was controlled by a syringe pump. Bright-field and fluorescence imaging were interlaced onto a single cooled electron-multiplied charge-coupled device (EMCCD) camera (Andor Ixon3 897). Fluorescence was excited at 488 nm by an argon ion laser (Lexel Laser) and controlled by a mechanical shutter. The bright field was illuminated by a transistor-transistor logic (TTL)-controlled light-emitting diode (Thorlabs).

Received 18 August 2013; accepted 18 March 2014;
published online 28 April 2014

References

- Chiu, S. The manipulation of neutral particles. *Rev. Mod. Phys.* **70**, 685–706 (1998).
- Forth, S., Sheinin, M., Inman, J. & Wang, M. Torque measurement at the single-molecule level. *Annu. Rev. Biophys.* **42**, 583–604 (2013).
- Moffitt, J. R., Chemla, Y. R., Smith, S. B. & Bustamante, C. Recent advances in optical tweezers. *Annu. Rev. Biochem.* **77**, 205–228 (2008).
- Hilario, J. & Kowalczykowski, S. C. Visualizing protein–DNA interactions at the single-molecule level. *Curr. Opin. Chem. Biol.* **14**, 15–22 (2010).
- Dholakia, K. & Cizmar, T. Shaping the future of manipulation. *Nature Photon.* **5**, 335–342 (2011).
- Padgett, M. & Bowman, R. Tweezers with a twist. *Nature Photon.* **5**, 343–348 (2011).
- Jannasch, A., Demirors, A. F., van Oostrum, P. D. J., van Blaaderen, A. & Schaffer, E. Nanonewton optical force trap employing anti-reflection coated, high-refractive-index titania microspheres. *Nature Photon.* **6**, 469–473 (2012).
- Grier, D. G. A revolution in optical manipulation. *Nature* **424**, 810–816 (2003).
- Fainman, Y., Psaltis, D. & Yang, C. *Optofluidics: Fundamentals, Devices, and Applications* Ch. 17 (McGraw-Hill, 2010).
- Erickson, D., Serey, X., Chen, Y. F. & Mandal, S. Nanomanipulation using near field photonics. *Lab on a Chip* **11**, 995–1009 (2011).
- Erickson, D., Rockwood, T., Emery, T., Scherer, A. & Psaltis, D. Nanofluidic tuning of photonic crystal circuits. *Opt. Lett.* **31**, 59–61 (2006).
- Diehl, L. *et al.* Microfluidic tuning of distributed feedback quantum cascade lasers. *Opt. Express* **14**, 11660–11667 (2006).
- Psaltis, D., Quake, S. R. & Yang, C. Developing optofluidic technology through the fusion of microfluidics and optics. *Nature* **442**, 381–386 (2006).
- Juan, M. L., Righini, M. & Quidant, R. Plasmon nano-optical tweezers. *Nature Photon.* **5**, 349–356 (2011).
- Schmidt, H. & Hawkins, A. R. The photonic integration of non-solid media using optofluidics. *Nature Photon.* **5**, 598–604 (2011).
- Fan, X. D. & White, I. M. Optofluidic microsystems for chemical and biological analysis. *Nature Photon.* **5**, 591–597 (2011).
- Molloy, J. E., Burns, J. E., Kendrick-Jones, J., Tregear, R. T. & White, D. C. Movement and force produced by a single myosin head. *Nature* **378**, 209–212 (1995).
- Farre, A., van der Horst, A., Blab, G. A., Downing, B. P. B. & Forde, N. R. Stretching single DNA molecules to demonstrate high-force capabilities of holographic optical tweezers. *J. Biophoton.* **3**, 224–233 (2010).
- Yang, A. H. J. *et al.* Optical manipulation of nanoparticles and biomolecules in sub-wavelength slot waveguides. *Nature* **457**, 71–75 (2009).
- Lin, S. Y. & Crozier, K. B. Planar silicon microrings as wavelength-multiplexed optical traps for storing and sensing particles. *Lab on a Chip* **11**, 4047–4051 (2011).
- Lin, S. Y. & Crozier, K. B. An integrated microparticle sorting system based on near-field optical forces and a structural perturbation. *Opt. Express* **20**, 3367–3374 (2012).
- Schmidt, B. S., Yang, A. H. J., Erickson, D. & Lipson, M. Optofluidic trapping and transport on solid core waveguides within a microfluidic device. *Opt. Express* **15**, 14322–14334 (2007).
- Mandal, S., Serey, X. & Erickson, D. Nanomanipulation using silicon photonic crystal resonators. *Nano Lett.* **10**, 99–104 (2010).
- Renaut, C. *et al.* On chip shapeable optical tweezers. *Sci. Rep.* **3**, 2290–2293 (2013).
- Jaquay, E., Martinez, L. J., Mejia, C. A. & Povinelli, M. L. Light-assisted, templated self-assembly using a photonic-crystal slab. *Nano Lett.* **13**, 2290–2294 (2013).
- Lei, T. & Poon, A. W. Silicon-on-insulator multimode-interference waveguide-based arrayed optical tweezers (SMART) for two-dimensional microparticle trapping and manipulation. *Opt. Express* **21**, 1520–1530 (2013).
- Soltani, M., Inman, J. T., Lipson, M. & Wang, M. D. Electro-optofluidics: achieving dynamic control on-chip. *Opt. Express* **20**, 22314–22326 (2012).
- Atabaki, A. H., Hosseini, E. S., Eftekhari, A. A., Yegnanarayanan, S. & Adibi, A. Optimization of metallic microheaters for high-speed reconfigurable silicon photonics. *Opt. Express* **18**, 18312–18323 (2010).
- Moffitt, J. R., Chemla, Y. R., Izhaky, D. & Bustamante, C. Differential detection of dual traps improves the spatial resolution of optical tweezers. *Proc. Natl Acad. Sci. USA* **103**, 9006–9011 (2006).
- Abbondanzieri, E. A., Greenleaf, W. J., Shaevitz, J. W., Landick, R. & Block, S. M. Direct observation of base-pair stepping by RNA polymerase. *Nature* **438**, 460–465 (2005).
- Sun, B. *et al.* ATP-induced helicase slippage reveals highly coordinated subunits. *Nature* **478**, 132–135 (2011).
- Forget, A. L., Dombrowski, C. C., Amitani, I. & Kowalczykowski, S. C. Exploring protein–DNA interactions in 3D using *in situ* construction, manipulation and visualization of individual DNA dumbbells with optical traps, microfluidics and fluorescence microscopy. *Nature Protoc.* **8**, 525–538 (2013).
- Gelles, J., Schnapp, B. J. & Sheetz, M. P. Tracking kinesin-driven movements with nanometre-scale precision. *Nature* **331**, 450–453 (1988).
- Fuller, D. N. *et al.* A general method for manipulating DNA sequences from any organism with optical tweezers. *Nucleic Acids Res.* **34**, e15–e24 (2006).
- Laib, S., Robertson, R. M. & Smith, D. E. Preparation and characterization of a set of linear DNA molecules for polymer physics and rheology studies. *Macromolecules* **39**, 4115–4119 (2006).

Acknowledgements

The authors thank members of the Wang Lab and the Lipson Lab for critical comments on this work. We especially thank J.L. Killian, L.D. Brennan, T. Roland, T.M. Konyakhina, and G.W. Feigenson for technical assistance. The authors acknowledge postdoctoral support to R.A.F. from the American Cancer Society (125126-PF-13-205-01-DMC), graduate traineeship support to S.N.S. from Cornell's Molecular Biophysics Training Grant funded by the National Institutes of Health (NIH, T32GM008267) and a National Science Foundation (NSF) Graduate Research Fellowship (grant no. DGE-1144153), and support to M.D.W. by the NIH (GM059849) and the NSF (MCB-0820293). This work was performed in part at the Cornell NanoScale Facility, a member of the National Nanotechnology Infrastructure Network, which is supported by the NSF (grant ECCS-0335765).

Author contributions

M.D.W. conceived the original concept for nSWAT and supervised the project. M.D.W. and M.S. collaborated on the experimental design and implementation. M.S. tested and optimized early prototypes of the nSWAT device. M.S. designed and simulated detailed features necessary to realize the current nSWAT implementation. M.S. and J.L. fabricated the devices with help from J.T.I., S.N.S. and M.L. J.L., R.A.F., M.S., J.T.I., S.N.S. and M.D.W. designed the measurement experiments. J.L., R.A.F., M.S. and S.N.S. performed the experiments with help from J.T.I., R.A.F., M.S. and J.L. analysed the data with help from S.N.S., J.T.I., J.L., R.A.F., M.S., S.N.S. and R.M.F. upgraded an existing measurement setup. M.D.W. and M.L. contributed materials/analysis tools. All authors contributed in drafting of the manuscript.

Additional information

Supplementary information is available in the [online version](#) of the paper. Reprints and permissions information is available online at www.nature.com/reprints. Correspondence and requests for materials should be addressed to M.D.W.

Competing financial interests

The authors declare no competing financial interests.